Development 138, 327-338 (2011) doi:10.1242/dev.057943

Bcl-2 proteins and autophagy regulate mitochondrial dynamics during programmed cell death in the *Drosophila* ovary

Elizabeth A. Tanner[1,2], Todd A. Blute[1], Carrie Baker Brachmann[3] and Kimberly McCall[1,*]

SUMMARY

The Bcl-2 family has been shown to regulate mitochondrial dynamics during cell death in mammals and *C. elegans*, but evidence for this in *Drosophila* has been elusive. Here, we investigate the regulation of mitochondrial dynamics during germline cell death in the *Drosophila melanogaster* ovary. We find that mitochondria undergo a series of events during the progression of cell death, with remodeling, cluster formation and uptake of clusters by somatic follicle cells. These mitochondrial dynamics are dependent on caspases, the Bcl-2 family, the mitochondrial fission and fusion machinery, and the autophagy machinery. Furthermore, Bcl-2 family mutants show a striking defect in cell death in the ovary. These data indicate that a mitochondrial pathway is a major mechanism for activation of cell death in *Drosophila* oogenesis.

KEY WORDS: *Drosophila*, Oogenesis, Programmed cell death, Mitochondria, Bcl-2, Autophagy, Apoptosis, Caspase, Mitochondrial fission and fusion

INTRODUCTION

In many organisms, cell death is essential for development and for tissue maintenance. Apoptosis, a major form of cell death, is controlled by evolutionarily conserved machinery that includes caspases, cysteine proteases that systematically dismantle the cell (Oberst et al., 2008). Mitochondria mediate major events of the apoptotic cascade in mammals. Healthy cells maintain a balance between pro- and anti-apoptotic factors, holding cell death at bay. When this balance is tipped toward apoptosis, Bcl-2 family proteins initiate mitochondrial remodeling, mitochondrial outer membrane permeabilization (MOMP), and the release of pro-apoptotic factors from the mitochondria (Wang and Youle, 2009).

Mitochondria exist as extensive networks that fragment early in the process of cell death in mammals (Suen et al., 2008). This process is facilitated by the Bcl-2 family proteins, which interact with the mitochondrial fission and fusion machinery to regulate mitochondrial network morphology in healthy and dying cells (Wang and Youle, 2009; Autret and Martin, 2010). Direct interactions between the Bcl-2 family proteins and the mitochondrial fission and fusion machinery are important for the induction of apoptosis. Upon initiation of apoptosis, the Bcl-2 family member Bax (Bcl-2-associated protein x) localizes to sites of fission on mitochondria with the mitochondrial fission protein Drp1 and the mitochondrial fusion protein Mitofusin 2 (Karbowski et al., 2002). Inactivation of Drp1 in cells undergoing apoptosis results in a delay in cytochrome c release from mitochondria (Autret and Martin, 2010). This suggests that an inhibition of mitochondrial fission can delay or prevent the induction of cell death. In agreement with this, if mitochondrial fusion is suppressed, sensitivity to cell death is increased (Autret and Martin, 2010). Furthermore, the mitochondrial fusion protein Opa1 is cleaved during apoptosis, disrupting cristae structure and releasing cytochrome c (Yamaguchi and Perkins, 2009). These findings suggest that mitochondrial remodeling is a pivotal event during cell death.

Mitochondrial regulation of cell death in *C. elegans* shares substantial similarity with mammals. The anti-apoptotic Bcl-2 protein CED-9 is localized to the mitochondria, and CED-9 interacts with the mitochondrial fusion machinery (Rolland et al., 2009). Activation of cell death induces Drp1-dependent mitochondrial fragmentation, and *drp1* mutants have decreased developmental cell death (Jagasia et al., 2005). Mitochondrial remodeling and localization of cell death factors to the mitochondria are shared characteristics central to the activation of cell death in mammals and worms. However, MOMP and cytochrome c release do not occur in *C. elegans*, suggesting that the evolutionarily conserved role for mitochondria in cell death extends beyond these factors (Oberst et al., 2008).

A growing body of evidence suggests that mitochondrial events play a role in promoting cell death in *Drosophila melanogaster* (Krieser and White, 2009). The major initiators of cell death are the IAP (inhibitor of apoptosis) binding proteins, Reaper, Hid (W – FlyBase), Grim and Sickle (Xu et al., 2009). These proteins mediate the inhibition and degradation of *Drosophila* inhibitor of apoptosis protein 1 (Diap1), a critical regulator of caspase activity (Orme and Meier, 2009). Many cell death regulators localize to the mitochondria, including the IAP-binding proteins, as well as the Bcl-2 family proteins Debcl and Buffy, the Apaf1 ortholog Ark, and the initiator caspase Dronc (Nc – FlyBase) (Krieser and White, 2009). Cytochrome c is unlikely to be a general activator of cell death in *Drosophila*, but it does play a role in certain contexts (Oberst et al., 2008; Krieser and White, 2009). Reaper and Hid have been shown

[1]Department of Biology, Boston University, Boston, MA 02215, USA. [2]Molecular Biology, Cell Biology, and Biochemistry Graduate Program, Boston University, Boston, MA 02215, USA. [3]Department of Developmental and Cell Biology, University of California, Irvine, CA 92697-2300, USA.

*Author for correspondence (kmccall@bu.edu)

Accepted 3 November 2010

to induce cytochrome c release, as well as mitochondrial remodeling in S2 cells (Abdelwahid et al., 2007). Mitochondrial remodeling also occurs during developmental cell death of larval tissues (Goyal et al., 2007). Furthermore, *Drosophila drp1* mutants are resistant to apoptosis induced by multiple stimuli (Abdelwahid et al., 2007).

In mammals and worms, the Bcl-2 family proteins regulate mitochondrial dynamics and control the initiation of cell death, but in *Drosophila* they have not been shown to regulate mitochondrial dynamics, and previous studies suggest that their role in cell death is surprisingly minor (Sevrioukov et al., 2007; Galindo et al., 2009; Wu et al., 2010). The two *Drosophila* Bcl-2 proteins, Buffy and Debcl, share the highest similarity with the mammalian Bcl-2 family protein Bok (Bcl-2 related ovarian killer) (Brachmann et al., 2000; Colussi et al., 2000; Igaki et al., 2000; Zhang et al., 2000). Mitochondrial dynamics are not altered in *debcl* mutants (Galindo et al., 2009). Interestingly, overexpression of *buffy* suppresses the phenotypes of *pink1*, a gene associated with Parkinson's disease that affects mitochondria (Park et al., 2006). In vitro studies and overexpression experiments in flies suggest that Buffy is anti-apoptotic and Debcl is pro-apoptotic (Quinn et al., 2003). Analysis of loss-of-function *buffy* and *debcl* mutants indicates little involvement in developmental cell death (Sevrioukov et al., 2007; Galindo et al., 2009), although Buffy has recently been shown to act pro-apoptotically during microchaete glial cell death (Wu et al., 2010). Additionally, both *buffy* and *debcl* mutants have been shown to regulate cell death in response to exogenous stimuli (Sevrioukov et al., 2007; Galindo et al., 2009). These findings indicate that *debcl* acts pro-apoptotically and *buffy* can act pro- or anti-apoptotically, depending on the context. However, any link with mitochondrial dynamics remains unclear.

An intriguing model for the investigation of a mitochondrial cell death pathway in *Drosophila* is the ovary (Pritchett et al., 2009; Xu et al., 2009). Cell death in the ovary occurs independently of the major initiators of cell death, Reaper, Hid and Grim (Foley and Cooley, 1998; Peterson et al., 2007). The *Drosophila* ovary contains egg chambers that progress through 14 defined stages of development (King, 1970). Each egg chamber consists of 15 nurse cells interconnected with one oocyte surrounded by hundreds of somatically derived follicle cells. During mid-oogenesis, prior to the energetically expensive process of vitellogenesis, a checkpoint acts to induce cell death in some of the egg chambers when nutrients are scarce (Drummond-Barbosa and Spradling, 2001). During this process, the nurse cell nuclei condense and fragment, follicle cells engulf the nurse cells, and then follicle cells are removed (Giorgi and Deri, 1976). The effector caspase Dcp-1 is essential for germline cell death at mid-oogenesis, but the pathway upstream of Dcp-1 remains unknown (Laundrie et al., 2003; Baum et al., 2007). The caspase inhibitor Diap1 is downregulated during this stage, lowering the threshold for Dcp-1 activation (Foley and Cooley, 1998; Baum et al., 2007). However, cell death occurs in only some of the egg chambers, suggesting that Diap1 downregulation is not sufficient and another factor is required for the activation of Dcp-1. A cascade of events centered around the mitochondria could be an alternative activation mechanism.

In this study, we have identified the mitochondrial events that occur during germline cell death in mid-oogenesis, and we have delineated the genetic pathway that controls these events. Nurse cell mitochondrial networks show extensive remodeling during cell death in the ovary, accompanied by cluster formation and engulfment by follicle cells. Both remodeling and cluster formation are inhibited by Diap1 overexpression. Notably, we find that the Bcl-2 family proteins Buffy and Debcl regulate mitochondrial remodeling and cell death during oogenesis. Furthermore, mutants of mitochondrial fission and fusion genes disrupt mitochondrial remodeling and cell death. Interestingly, we found a role for the autophagic machinery in mitochondrial maintenance, as well as uptake of the cytoplasm and mitochondrial clusters by the surrounding follicle cells during cell death. These data indicate that a mitochondrial pathway is a major mechanism for activation of cell death in *Drosophila* mid-oogenesis.

MATERIALS AND METHODS

Drosophila strains

Fly strains used in this study included w^{1118}, *UASp-mitoGFP* and *w; NGT; nosGAL4::VP16* (Cox and Spradling, 2003); $atg1^{\Delta 3D}$ (Scott et al., 2007), $atg7^{d77}$and $atg7^{d14}$ (Juhasz et al., 2007); *mcherry-Dratg8a* (Nezis et al., 2009); $buffy^{H37}$, $debcl^{E26}$ and *w;* $buffy^{H37}$*; da-GAL4 UASt-buffy/TM6B* (Sevrioukov et al., 2007); $drp1^{1}$and $drp1^{2}$ (Verstreken et al., 2005); *opa1-like*^{EY09863} (FlyBase); *dcp-1*^{prev1} (Laundrie et al., 2003); *UASp-diap1* (Peterson et al., 2003); and *UASp-p35* (Baum et al., 2007). Of these mutants, the *atg1*, *atg7*, *buffy* and *dcp-1* mutants have been described as null. The *debcl* and *opa1-like* mutants are likely to be strong hypomorphs. $drp1^{1}$and $drp1^{2}$ are strong loss-of-function or null alleles. Flies were obtained from the laboratories that generated the strains or from the Bloomington Stock Center. All flies were cultured at 25°C on standard cornmeal-molasses medium. Germline clones were generated using the *HS-FLP; FRT ovo*^{D} method as described previously (Baum et al., 2007).

Ovary dissection and staining

Flies were conditioned on yeast paste for 2 days followed by starvation for 1-2 days on apple juice agar. Ovaries were dissected in room-temperature PBS followed by LysoTracker (Invitrogen) staining, antibody staining and/or DNA staining. Double labeling for LysoTracker and anti-ATP synthase was performed as described (Frydman and Spradling, 2001; Bass et al., 2009) with a modified fixation (4% paraformaldehyde in Graces medium with a half volume heptane for 20 minutes at room temperature). Primary antibodies were: anti-ATP synthase (1:1000; mitoSciences), anti-discs large (1:1000; Developmental Studies Hybridoma Bank) and anti-*Drosophila* e-cadherin, Dcad2 (1:10; Developmental Studies Hybridoma Bank). Secondary antibodies used were goat anti-mouse Cy3 (1:200) and goat anti-rat DyLight 649 (1:200) (both from Jackson ImmunoResearch), goat anti-mouse AlexaFluor 488 (1:500) and goat anti-mouse AlexaFluor 633 (1:500) (both from Invitrogen). For OliGreen nuclear stain (Molecular Probes), samples were incubated with OliGreen (1:5000) in PBS with 200 μg/ml RNase A for 30 minutes at room temperature. For propidium iodide staining, samples were incubated in 600 μg/ml RNase A in PBS for 1 hour at room temperature, followed by incubation in 1 mg/ml propidium iodide in PBS for 1 hour at room temperature.

Microscopy

All images were taken on a Zeiss LSM510 confocal microscope, with the exception of DAPI images. Images were taken with a 63× oil lens and a pinhole diameter of 1 airy unit was used for all confocal acquisition. DAPI images were taken with an Olympus BX51 microscope with DSU spinning disk attachment using a 40× water-immersion lens. The egg chambers that were imaged ranged from stage 7 to 9 of oogenesis, the stages when degeneration normally occurs. To determine the nature of the mitochondrial networks, a series of *z* sections for each egg chamber was taken at 1 μm intervals for an average of 15 sections. The mitochondrial network morphology was analyzed in all *z* sections and scored as healthy (H), normally degenerating (N) or abnormal (A). The line scan plot was generated using LSM510 software. Electron microscopy was performed as described previously (Bass et al., 2009). Prior to post-fix, egg chambers were identified as degenerating using light microscopy.

RESULTS

Mitochondrial clustering occurs during cell death in mid-oogenesis

To determine whether mitochondrial remodeling is associated with cell death in *Drosophila* mid-oogenesis, we visualized mitochondrial networks in wild-type flies using a mitochondria-

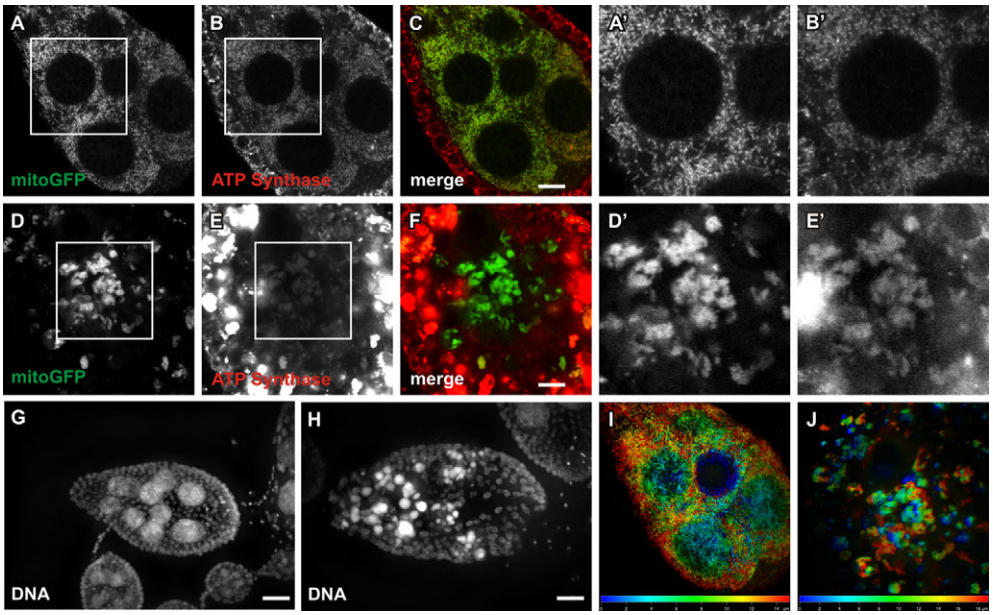

Fig. 1. Mitochondrial clustering occurs during cell death in mid-oogenesis. (A-F) Single *z* plane images through the egg chambers. (**A-C**) Mitochondrial network in a healthy egg chamber labeled with (A) *mitoGFP*, (B) anti-ATP synthase antibody and (C) merge showing colocalization. *UASp-mitoGFP* was driven by the germline-specific *NGT;nosGAL4*, which expresses only in the germline tissue and not in the surrounding somatic follicle cells. (**A′**,**B′**) Boxed regions from A and B at 252× zoom. (**D-F**) Mitochondrial network in dying egg chamber with (D) *mitoGFP*, (E) anti-ATP synthase and (F) merge. (**D′**,**E′**) Boxed regions from D and E at 252× zoom. Brightness was increased in E to show signal within the nurse cells. (**G**,**H**) Egg chambers shown in A-F stained with DAPI to reveal nuclear morphology. Images are projections of several *z* planes. (**I**,**J**) Depth-coded projection images of the green channel from the egg chambers in A and D. Confocal *z* planes are assigned a color determined by the depth of the section in the projection: blue sections are at the top of the egg chamber, whereas red sections are deepest into the egg chambers. Scale bars: 10 μm.

localized GFP (Cox and Spradling, 2003) and an anti-ATP synthase antibody. Healthy egg chambers displayed mitochondria throughout the egg chamber (Fig. 1A-C). The germline specific mitoGFP and the anti-ATP synthase staining overlay within the germline, validating mitochondrial detection (Fig. 1C). To induce cell death in mid-oogenesis, flies were nutrient deprived by shifting to media lacking a protein source. We found that the mitochondrial networks showed distinct changes during cell death. Nurse cell mitochondria formed clusters, as seen with mitoGFP (Fig. 1D) and anti-ATP synthase (Fig. 1E). Interestingly, ATP synthase levels increased dramatically in the surrounding follicle cells compared with the degenerating nurse cells. To determine the three dimensional nature of the networks observed, we created depth coded projection images of confocal *z* sections for the mitoGFP (green channel). Mitochondrial networks in healthy egg chambers showed extensive tubular networks (Fig. 1I), while degenerating egg chambers showed clusters (Fig. 1J).

In degenerating egg chambers, the mitoGFP clusters were seen in both the nurse cells and follicle cells, suggesting that the germline mitochondrial clusters were engulfed by the surrounding follicle cells. To characterize fully the changes occurring during cell death and to determine which events occur in the nurse cells as opposed to the follicle cells, we analyzed a series of egg chambers for sequential changes in nuclear morphology, mitochondrial networks and follicle cell membrane morphology. Healthy egg chambers showed large uncondensed nurse cell nuclei, mitochondrial networks throughout the nurse cells, and a regular pattern of follicle cell membranes surrounding the nurse cells (Fig. 2A-D). Egg chambers early in the death process, as determined by partially condensed nuclei, showed generally disrupted mitochondrial networks with some punctate mitochondria and small clusters (Fig. 2E-H). Membrane staining revealed clusters of mitochondria that were taken up by the surrounding follicle cells (Fig. 2H). Later in the cell death process, nurse cell nuclei were condensed and fragmented, the mitochondria formed clusters and the follicle cell volume increased (Fig. 2I-L). Large pieces of fragmented nurse cell nuclei, as well as many mitochondrial clusters were taken up into the follicle cells (Fig. 2L) (Giorgi and Deri, 1976). In an egg chamber with few nurse cell nuclear remnants, mitochondrial clusters persisted, but these were primarily in the follicle cells (Fig. 2M-P). After the nurse cell nuclei were degraded and only follicle cell nuclei remained, the mitoGFP-labeled mitochondria were no longer detectable, and the follicle cell membrane staining was lost (Fig. 2Q-T). This progression of mitochondrial network breakdown and clustering, along with uptake by the surrounding follicle cells suggests that germline mitochondria undergo four major events during cell death in mid-oogenesis: (1) remodeling that may be fragmentation, (2) clustering, (3) uptake by the surrounding follicle cells, and (4) degradation in the follicle cells.

Mitochondrial clustering is dependent on caspase activity

Mitochondrial events, including remodeling, generally occur prior to caspase activation in mammals and *C. elegans*, and are sufficient to induce cell death (Suen et al., 2008). To determine whether mitochondrial changes occur prior to caspase activation during cell death in mid-oogenesis, we analyzed mitochondrial networks in caspase-deficient egg chambers. Germline cell death in mid-oogenesis is dependent upon the effector caspase Dcp-1 (Laundrie

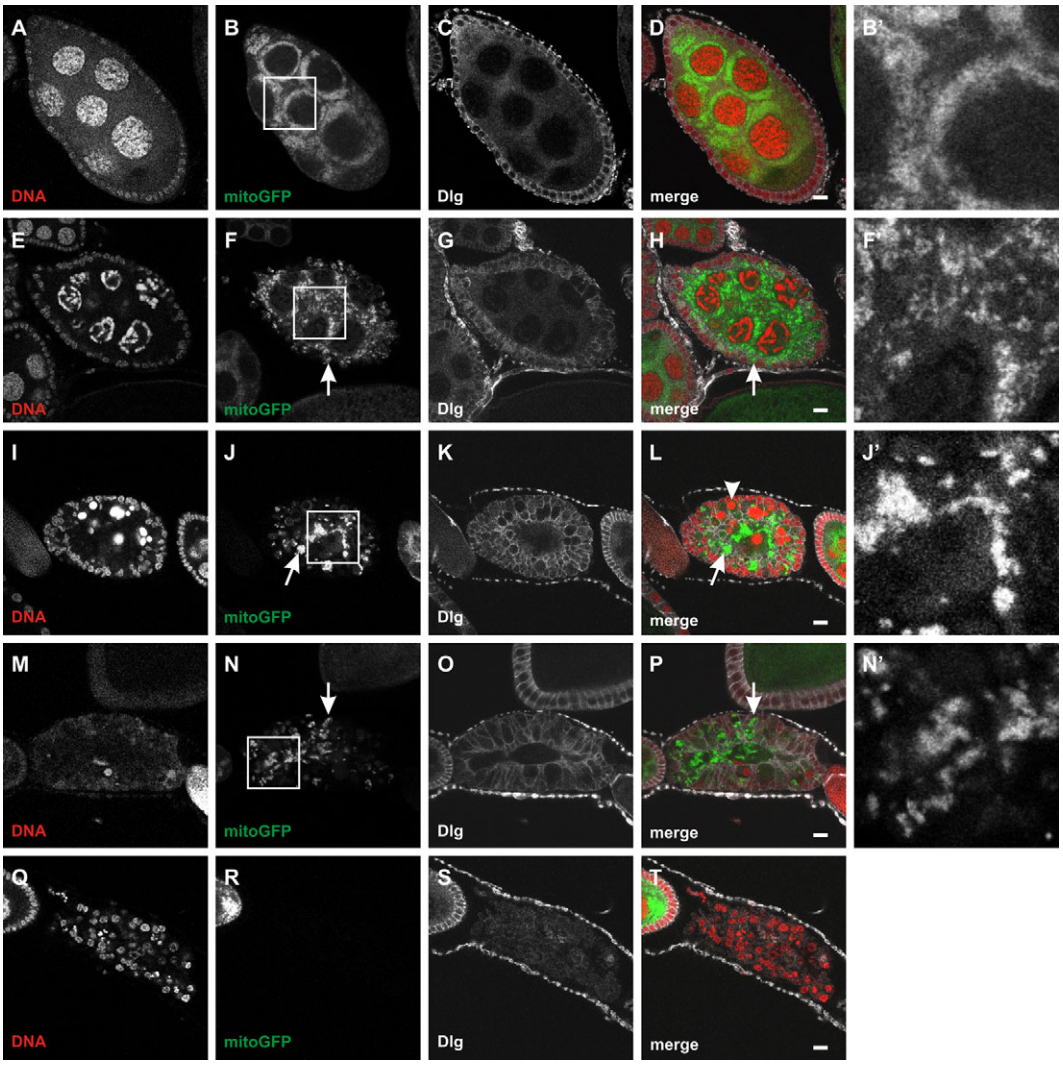

Fig. 2. Wild-type egg chambers show mitochondrial clustering and uptake into follicle cells during cell death in mid-oogenesis. (**A-D**) A healthy egg chamber. (**E-H**) An egg chamber early in the cell death process. (**I-L**) An egg chamber midway through degeneration. (**M-P**) An egg chamber late in the cell death process. (**Q-T**) Follicle cells remaining after nurse cells are gone. Arrows indicate mitochondrial clusters within the follicle cells. Arrowhead in L indicates nurse cell nuclear fragment in follicle cell. (**B′**,**F′**,**J′**,**N′**) Boxed regions from B,F,J,N at 252× zoom. For all samples, DNA is stained with propidium iodide (red), mitochondria are labeled with *mitoGFP* (green) and membranes are stained with anti-Discs large (Dlg, white). Scale bars: 10 μm.

et al., 2003; Baum et al., 2007). In *dcp-1*^{Prev1} mutants, degeneration does not occur normally, and mid-stage egg chambers exhibit a phenotype in which the follicle cells disappear prematurely and only the nurse cells and oocyte remain (Fig. 3I). This phenotype suggests that egg chambers have received a cell death signal that results in the disappearance of the somatically derived follicle cells. However, disruption of *dcp-1* prevents germline cell death from proceeding and the egg chambers remain in an 'undead' state. Analysis of mitochondria in *dcp-1* undead egg chambers showed abnormal mitochondrial networks (Fig. 3J-K). The *dcp-1* mitochondria showed some remodeling but very little clustering. This suggests that mitochondrial remodeling occurs upstream of Dcp-1 activity while clustering occurs downstream.

To quantify the changes we observed in mitochondrial networks, we scored egg chambers using the following criteria. Analysis of mitochondrial networks showed that wild-type healthy egg chambers consistently displayed the pattern shown in Fig. 3B. These ubiquitous networks were designated as healthy (H) (Fig. 3D). Degenerating wild-type egg chambers showed the pattern of remodeling and clustering shown in Fig. 3F, and these were designated as normal degenerating (N) (Fig. 3H). Mitochondrial networks that did not fall into these categories were designated as abnormal (A). *dcp-1* undead egg chambers had variable mitochondrial patterns that appeared fragmented, irregular or overly connected, and often these patterns occurred within the same egg chamber. For example, Fig. 3J shows an egg chamber with two different regions of mitochondrial patterning. Overall, 89% of *dcp-1* undead egg chambers showed abnormal networks (Fig. 3L).

Because *dcp-1* mutants exhibited a partial inhibition of mitochondrial changes, we reasoned that other caspases could be contributing to mitochondrial events. Therefore, we examined egg chambers overexpressing the caspase inhibitors *p35* and *diap1* in the germline. Overexpression of the caspase inhibitors *p35* or *diap1* results in the same undead phenotype where all germline mid-stage cell death is blocked (Peterson et al., 2003; Mazzalupo and Cooley, 2006; Baum et al., 2007). *p35*-expressing undead egg chambers

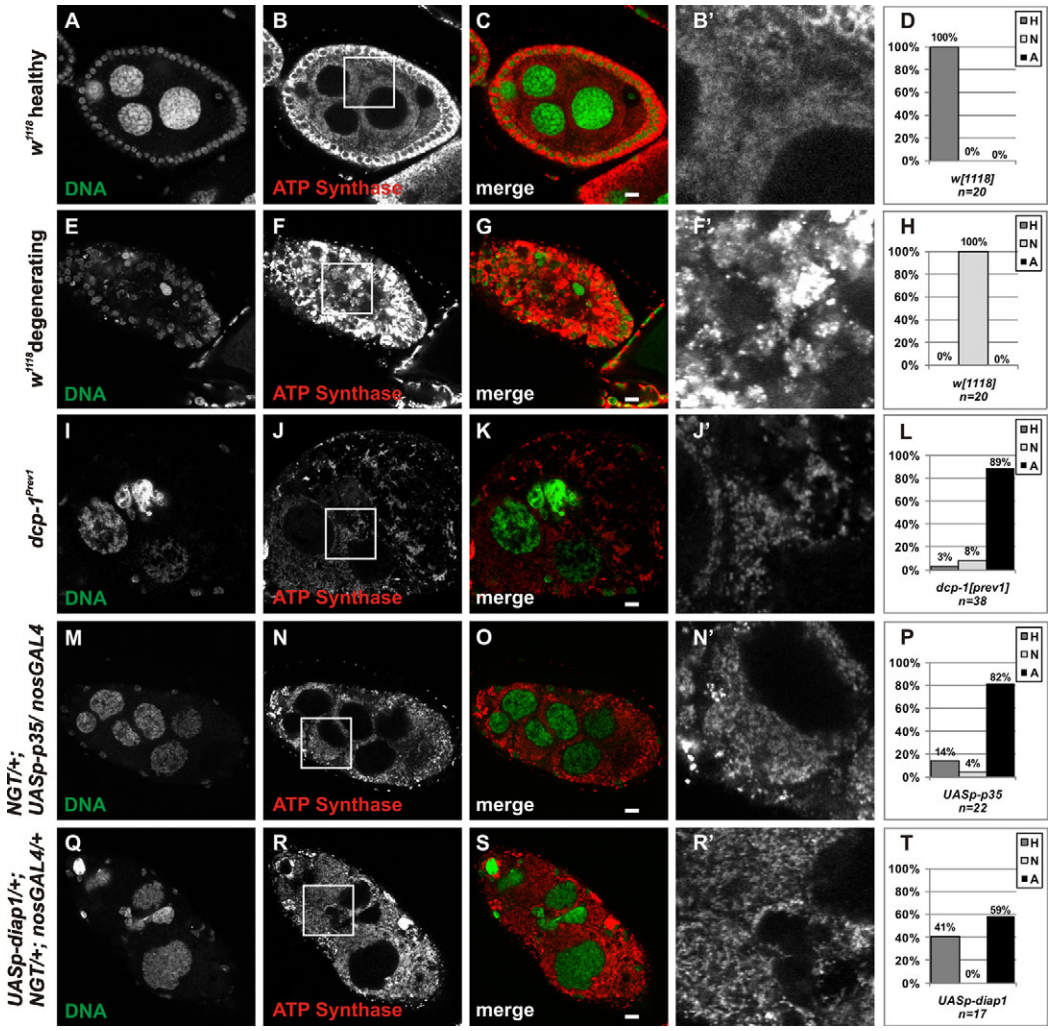

Fig. 3. Caspase inhibition disrupts mitochondrial remodeling. (**A-C**) A control healthy egg chamber. (**E-G**) A control degenerating egg chamber. (**I-K**) A *dcp-1*^{prev1} undead egg chamber. (**M-O**) An undead egg chamber overexpressing *p35* in the germline *(NGT/+;UASp-p35/nosGAL4)*. (**Q-S**) An undead egg chamber overexpressing *diap1* in the germline *(UASp-diap1/+;NGT/+;nosGAL4/+)*. All samples show nuclear morphology (DNA, OliGreen), mitochondrial morphology (anti-ATP synthase, red) and merge. All images are single *z* planes. Scale bars: 10 μm. (**B′**,**F′**,**J′**,**N′**,**R′**) Boxed regions from B,F,J,N,R at 252× zoom. (**D**,**H**,**L**,**P**,**T**) Quantification of mitochondrial network patterns. Data are percentage of egg chambers showing the following mitochondrial network patterns: H, healthy networks as seen in healthy wild-type egg chambers; N, normal degeneration as seen in degenerating wild-type egg chambers; A, abnormal mitochondrial networks; *n*, the number of egg chambers analyzed.

showed mitochondrial network disruptions (Fig. 3M-P) similar to the *dcp-1* mutant (Fig. 3I-L). However, *diap1* overexpression led to a more significant block and 41% of the undead egg chambers showed completely unchanged mitochondrial networks (Fig. 3Q-T), resembling networks seen in healthy wild-type egg chambers. The remainder of the egg chambers looked similar to the abnormal egg chambers in *dcp-1* mutants. The more robust inhibition by *diap1* compared with *p35* or *dcp-1* mutants could be because Diap1 inhibits the initiator caspase Dronc as well as effector caspases. Thus, Dronc or another Diap1 target could control mitochondrial remodeling.

diap1 overexpression resulted in a mixed phenotype, with undead egg chambers displaying either healthy or abnormal mitochondrial networks. To determine whether the abnormal mitochondrial network phenotype was a secondary consequence of being in the undead state, we examined the progression of the undead egg chambers. With caspase inhibition in the ovary, undead egg chambers accumulate in succession with prolonged starvation (data not shown). Therefore, we scored the egg chambers for anterior positioning next to a healthy egg chamber and the state of their mitochondrial networks. All egg chambers with healthy mitochondria were located anteriorly, and the more posterior egg chambers had the most abnormal mitochondrial morphology (data not shown). This suggests that the healthy networks in Diap1-inhibited egg chambers eventually progress to an abnormal state.

Bcl-2 mutants partially inhibit germline cell death and show abnormal mitochondrial remodeling

The principal initiators of cell death in most *Drosophila* tissues, *reaper*, *hid* and *grim*, are not involved in germline cell death (Foley and Cooley, 1998; Peterson et al., 2007); therefore, we wished to identify the upstream cell death regulators that control the dramatic mitochondrial remodeling observed during cell death in mid-oogenesis. Bcl-2 family proteins regulate the activation of cell death through modulation of mitochondrial events in mammals and *C. elegans* (Wang and Youle, 2009), and are interesting candidates

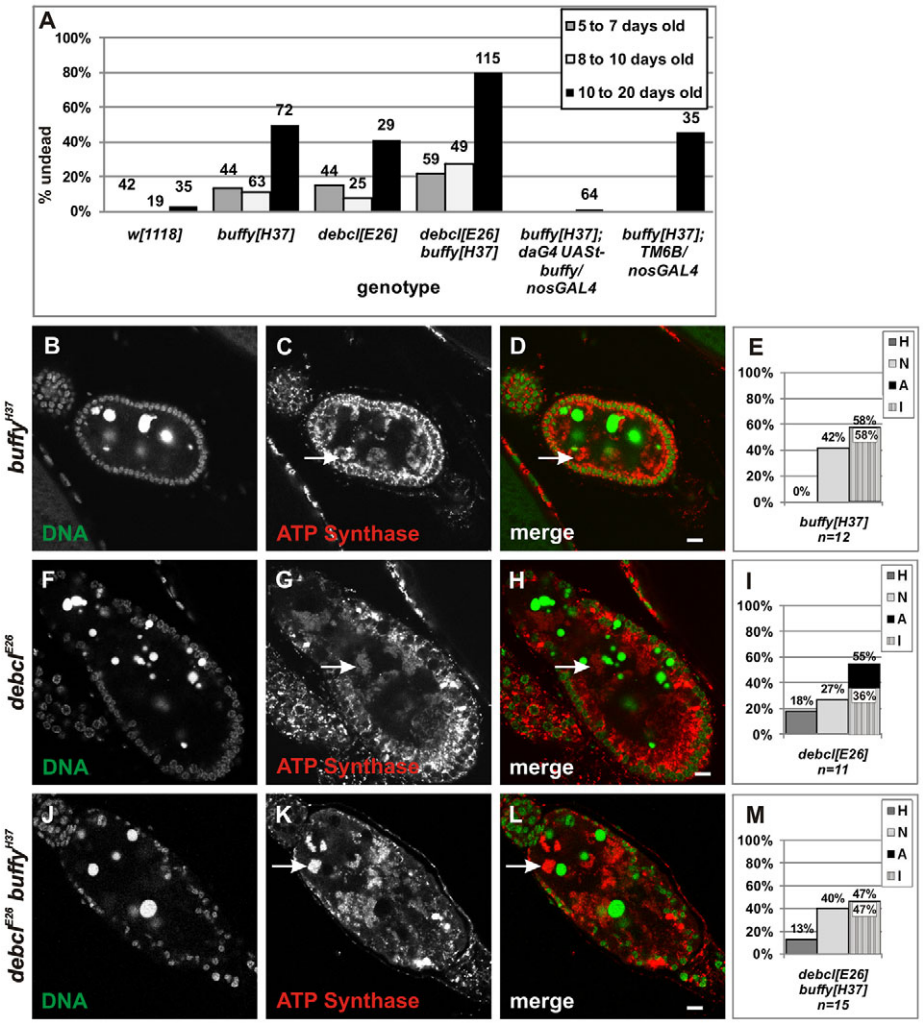

Fig. 4. Abnormal mitochondrial networks in degenerating egg chambers of Bcl-2 family mutants. (**A**) Quantification of undead egg chambers compared with normal degeneration. Number of egg chambers scored is indicated above the columns. Data are percentage of undead egg chambers. (**B-D**) A *buffy*^{H37} degenerating egg chamber. (**F-H**) A *debcl*^{E26} degenerating egg chamber. (**J-L**) A *debcl*^{E26}*buffy*^{H37} degenerating egg chamber. All samples show nuclear morphology (DNA, OliGreen), mitochondrial morphology (anti-ATP synthase, red) and merge. Arrows indicate mitochondrial islands. Scale bars: 10 μm. (**E**,**I**,**M**) Quantification of mitochondrial network patterns. Data are percentage of degenerating egg chambers showing the following mitochondrial network paterns: H, healthy networks as seen in healthy wild-type egg chambers; N, normal degeneration as seen in degenerating wild-type egg chambers; A, abnormal mitochondrial networks; I, abnormal networks with mitochondrial islands; *n*, the number of egg chambers analyzed.

for regulating cell death in mid-oogenesis. To determine whether the Bcl-2 family proteins contribute to the activation of cell death during mid-oogenesis, we analyzed mutants of *debcl* and *buffy*, as well as a double mutant. *debcl*^{E26} and *buffy*^{H37} mutants showed an inhibition in cell death, where some egg chambers had the undead phenotype (Fig. 4A; see Fig. S1 in the supplementary material). A rescue construct for *buffy* abrogated the undead phenotype (Fig. 4A; see Fig. S1F in the supplementary material). The double mutant *debcl*^{E26}*buffy*^{H37} also had a significant number of egg chambers with the undead phenotype; the occurrence of undead egg chambers was greater in the double mutant than in either of the individual mutants, suggesting that both *debcl* and *buffy* act pro-apoptotically. Interestingly, the percentage of undead egg chambers increased as the flies aged (Fig. 4A). In the double mutant, as many as 80% of the egg chambers were undead. Therefore, the Bcl-2 family proteins regulate mid-oogenesis cell death, and the effect is more prominent in older flies.

To determine if *debcl* and *buffy* regulate mitochondrial remodeling during cell death in mid-oogenesis, we investigated the mitochondrial morphology in egg chambers. Healthy egg chambers from the Bcl-2 family mutants showed only subtle differences from wild type (data not shown). Interestingly, in many mutant egg chambers undergoing normal degeneration, as determined by nurse cell nuclear morphology, we observed abnormal mitochondrial remodeling with large masses of mitochondria that we termed ‘islands’ (Fig. 4). The mitochondrial islands were distinct from clusters seen during wild-type degeneration in that islands were larger mitochondrial structures that were separate from surrounding mitochondria. Overall, 53% of degenerating egg chambers from the Bcl-2 family mutants showed abnormal networks, with 47% showing mitochondrial islands (Fig. 4E,I,M). In undead egg chambers from *buffy*, *debcl* and *debcl buffy* double mutants, the mitochondrial networks were mostly healthy, or abnormal (Fig. 5), similar to what was seen with *diap1* overexpression. Only a minority of the Bcl-2 family mutant egg chambers showed normally degenerating mitochondrial networks, as seen in wild type. These findings indicate that the Bcl-2 family proteins regulate mitochondrial dynamics during cell death in oogenesis.

Disruption of mitochondrial fission and fusion results in abnormal mitochondrial remodeling and cell death inhibition

To investigate whether the mitochondrial fission and fusion machinery regulates mid-oogenesis cell death, we analyzed mutants of the mitochondrial fission protein Drp1 and the mitochondrial fusion protein Opa1. Because mutations in both genes are homozygous lethal, germline clones (GLCs) were analyzed. In healthy *drp1*^{1} and *drp1*^{2} mutant egg chambers, mitochondrial networks showed an overly connected appearance, consistent with a disruption of mitochondrial fission (see Fig. S2A-C in the supplementary material; data not shown). Interestingly,

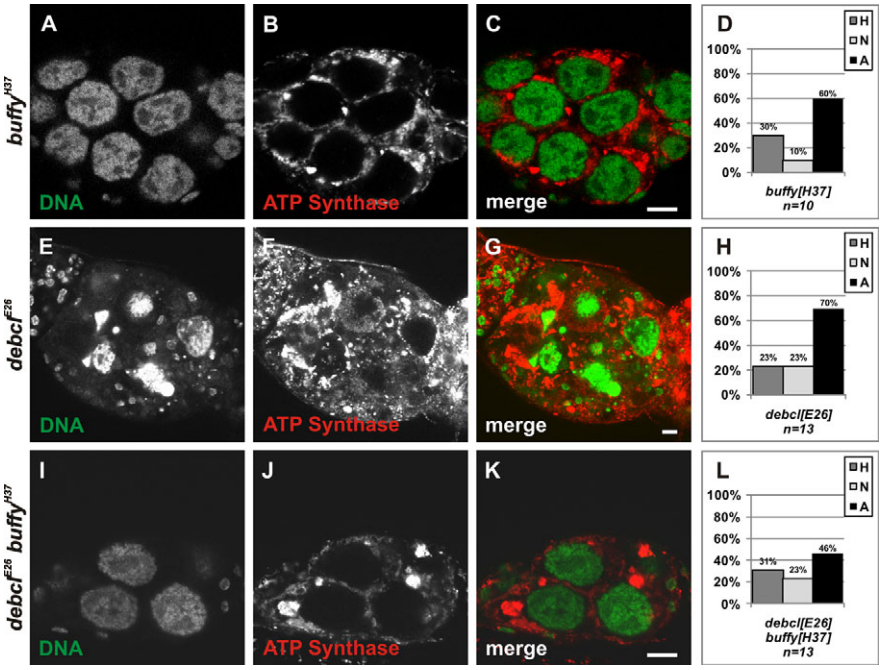

Fig. 5. *buffy* and *debcl* mutants have abnormal mitochondrial networks in undead egg chambers. (**A-C**) A *buffy*^{H37} undead egg chamber. (**E-G**) A *debcl*^{E26} undead egg chamber. (**I-K**) A *debcl*^{E26}*buffy*^{H37} undead egg chamber. All samples show nuclear morphology (DNA, OliGreen), mitochondrial morphology (anti-ATP synthase, red) and merge. Scale bars: 10 μm. (**D**,**H**,**L**) Quantification of mitochondrial network patterns. Data are the percentage of undead egg chambers showing the following mitochondrial network patterns: H, healthy networks as seen in healthy wild-type egg chambers; N, normal degeneration as seen in degenerating wild-type egg chambers; A, abnormal mitochondrial networks; *n*, the number of egg chambers analyzed.

nuclear morphology was also affected in these mutants. Wild-type nurse cell nuclei have condensed polytene chromosomes in early stages of oogenesis, but the chromosomes disperse by stage 6 (see Fig. S3 in the supplementary material) (Dej and Spradling, 1999). In *drp1* GLCs, the polytene chromosomes were not dispersed by stage 8 and occasionally polytene chromosomes persisted into late oogenesis (see Fig. S3C in the supplementary material). In addition, we analyzed *opa1-like* by both loss-of-function and overexpression analyses. Mitochondrial networks in healthy egg chambers from *opa1-like*^{EY09863} GLCs appeared less tubular than wild type, as would be expected from a disruption in fusion (see Fig. S2D-F in the supplementary material). Overexpression of *opa1-like* caused variable mitochondrial network morphologies (see Fig. S2G-I in the supplementary material), but some of the egg chambers (37%, *n*=8) had overly connected mitochondrial networks similar to the *drp1* mutants.

To determine how mitochondrial remodeling was affected during cell death, mitochondrial networks in degenerating egg chambers were analyzed. *drp1* GLCs had abnormal mitochondrial networks in degenerating egg chambers with mitochondrial islands present in 80% of egg chambers (Fig. 6A-D). *opa1-like* GLCs showed a variable phenotype with healthy, normal degenerating and abnormal mitochondrial networks (Fig. 6E-H), whereas *opa1-like* overexpression caused abnormal mitochondrial remodeling with islands in the majority of egg chambers (Fig. 6I-L), similar to *drp1* GLCs.

Disruption of mitochondrial fission and fusion has been shown to affect the sensitivity of cells to apoptotic stimuli; therefore, we analyzed *drp1* and *opa1-like* mutants to determine whether they affected cell death in mid-oogenesis. *drp1* GLCs showed an inhibition in cell death with some undead egg chambers (Fig. 6M). Similarly, GLCs and overexpression of *opa1-like* had some undead egg chambers present (Fig. 6M). Overexpression of *opa1-like* showed an increase in the undead phenotype in an age-dependent manner (Fig. 6N) similar to Bcl-2 family mutants. This suggests that mitochondrial fission and fusion are involved in the activation of cell death in mid-oogenesis.

Mitochondrial dynamics are abnormal in autophagy deficient egg chambers

Autophagy plays an important role in mitochondrial turnover and can also act as a cell death mechanism (Twig et al., 2008; Goldman et al., 2010). Autophagy is induced downstream of the effector caspase *dcp-1* during cell death in mid-oogenesis (Velentzas et al., 2007; Hou et al., 2008; Nezis et al., 2009). To determine whether the mitochondrial clusters in dying egg chambers are a result of autophagic sequestration of the mitochondria, we analyzed mitochondrial networks in mutants of *atg1*, a key regulator of autophagy (Scott et al., 2007). *atg1* mutants are homozygous lethal and GLCs of the allele *atg1*$^{\Delta 3d}$ were created for analysis. Healthy *atg1* GLC egg chambers showed abnormal mitochondrial networks (Fig. 7A-E) that appeared to be more connected than wild-type, and dying egg chambers had abnormal mitochondrial remodeling that included the presence of islands (Fig. 8A-D,M). Egg chambers early in degeneration had healthy mitochondrial networks, even though nuclear condensation and fragmentation progressed (data not shown). Egg chambers later in degeneration, as determined by nuclear morphology, formed mitochondrial islands (Fig. 8C). Furthermore, out of 11 egg chambers analyzed, three showed a striking delay in uptake by the surrounding follicle cells (Fig. 8B), and two of the egg chambers analyzed had large regions of irregular follicle cell morphology.

To determine whether similar changes were seen in other autophagy mutants, a homozygous viable allelic combination of *atg7* was analyzed (Juhasz et al., 2007). In the *atg7*^{d77}/*atg7*^{d14} transheterozygotes, healthy egg chambers had abnormal mitochondrial patterns like *atg1* GLCs (Fig. 7F-J). Early degenerating *atg7* egg chambers showed healthy mitochondrial networks, whereas nurse cell nuclear condensation and fragmentation proceeded, similar to *atg1* GLCs. Egg chambers further along in degeneration appeared similar to wild-type, and none of the egg chambers we analyzed showed a delay in uptake by the follicle cells, in contrast to *atg1* GLCs. However, the size of the mitochondrial clusters and the follicle cell morphology differed

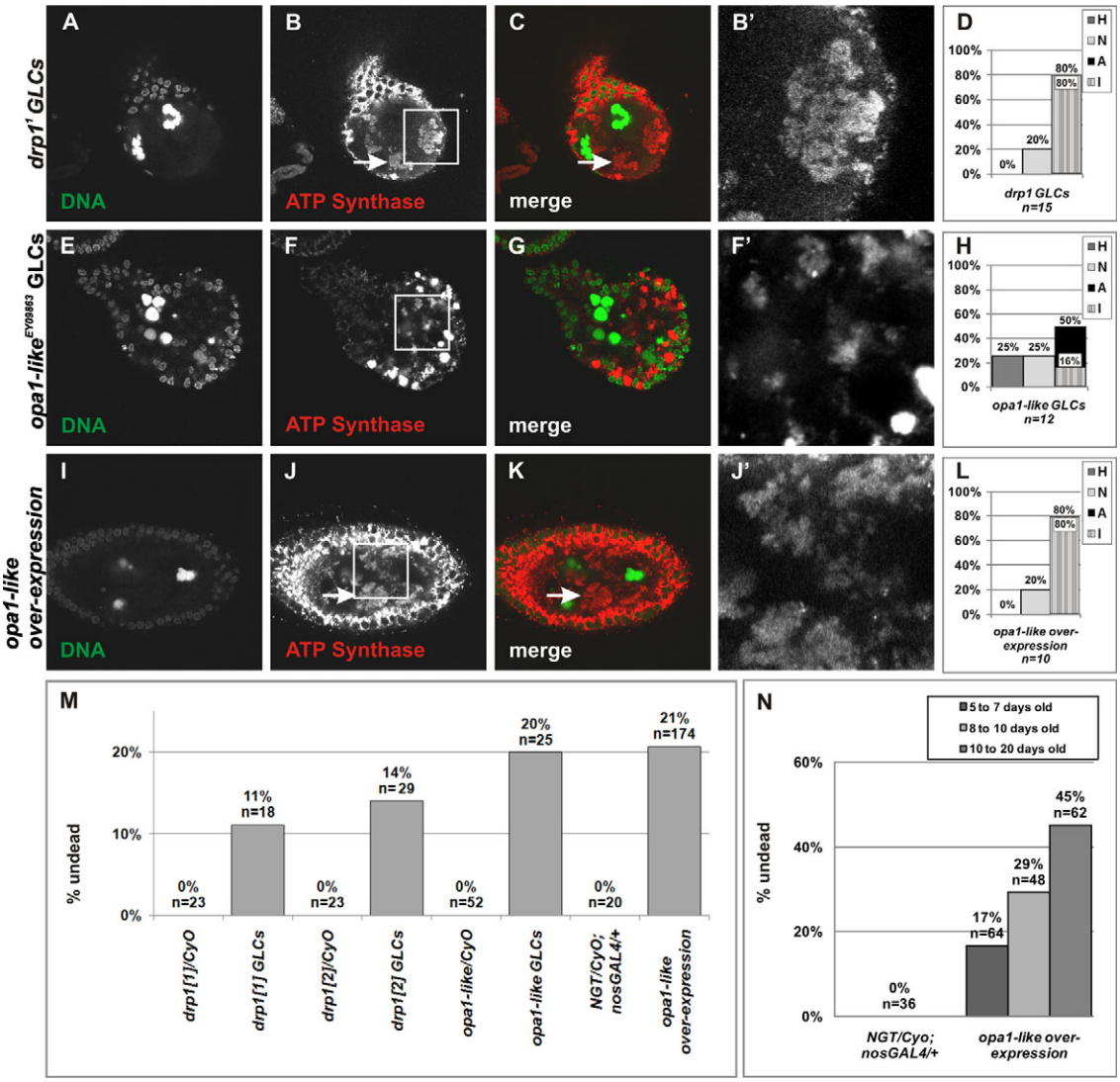

Fig. 6. *drp1* and *opa1-like* mutants have abnormal mitochondrial remodeling during cell death in mid-oogenesis. (**A-C**) A *drp1*^{1} GLC degenerating egg chamber. Egg chamber is surrounded by follicle cells but they are not apparent in this *z* plane. (**D**) Quantification of mitochondrial network patterns in *drp1*^{1} and *drp1*^{2} GLCs. (**E-G**,**H**) An *opa1-like*^{EY09863} GLC degenerating egg chamber and quantification. (**I-K**,**L**) Overexpression of *opa1-like* in a degenerating egg chamber and quantification. All samples show nuclear morphology (DNA, OliGreen), mitochondrial morphology (anti-ATP synthase, red) and merge. Mitochondrial islands are indicated by arrows. (**B′**,**F′**,**J′**) Boxed regions from B,F,J at 252× zoom. (D,H,L) Quantification of mitochondrial network patterns. Data are the percentage of degenerating egg chambers showing the following mitochondrial network patterns: H, healthy networks as seen in healthy wild-type egg chambers; N, normal degeneration as seen in degenerating wild-type egg chambers; A, abnormal mitochondrial networks; I, abnormal networks with mitochondrial islands; *n*, the number of egg chambers analyzed. (**M**) Quantification of undead egg chambers. Data are the percentage of undead egg chambers. (**N**) Age dependence of undead phenotype with *opa1-like* overexpression. The control egg chambers were from *NGT/CyO; nosGAL4/+* siblings from the oldest cohort. *n*, the number of egg chambers scored.

from wild-type. *atg7* follicle cells contained larger clusters of mitochondria than did wild type, and follicle cell membranes had large irregular regions (Fig. 8E-H,N), similar to *atg1* GLCs. These observations suggest that autophagy contributes to uptake and degradation of the mitochondria by the surrounding follicle cells, as well as mitochondrial maintenance in healthy egg chambers and remodeling during cell death.

To examine whether the autophagic machinery contributes directly to mitochondrial remodeling and uptake, we analyzed expression of *mcherry-Dratg8a* (Nezis et al., 2009) and *mitoGFP* in the germline. Atg8 protein fusions have been used to detect autophagosomes and autolysosomes in many systems. Atg8 is cytoplasmic in healthy tissue and becomes punctate upon induction of autophagy, probably at the site of autophagosome formation. We found that the mCherry-DrAtg8a signal was generally found throughout the cytoplasm in healthy and degenerating wild-type egg chambers. We saw very little punctate mCherry-DrAtg8a signal, in either healthy or degenerating egg chambers, and the puncta did not colocalize with mitochondrial clusters. Mitochondria were taken up by the surrounding follicle cells and the engulfed cytoplasm contained both the mCherry-DrAtg8a reporter, as well as mitoGFP (Fig. 8I-L). Importantly, the majority of colocalization between the reporters was in the follicle cells (Fig. 8L, inset; Fig. 8O). Some of the egg chambers (33.3%, *n*=15) showed large

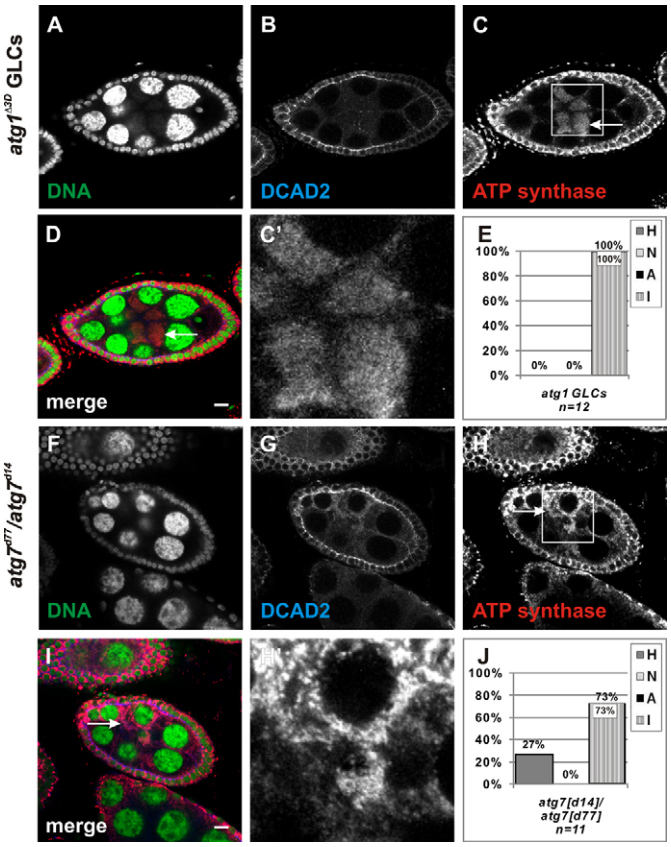

Fig. 7. *atg1* and *atg7* mutants have abnormal mitochondrial networks in healthy egg chambers. (**A-D**) A healthy $atg1^{\Delta 3D}$ GLC egg chamber. (**F-I**) An $atg7^{d77}/atg7^{d14}$ egg chamber. Samples show nuclear morphology (DNA, OliGreen), follicle cell membrane staining (anti-*Drosophila* e-cadherin DCAD2, blue), mitochondrial morphology (anti-ATP synthase, red) and merge. Mitochondrial islands are indicated by arrows. (**C′**,**H′**) Boxed regions from C and H at 252× zoom. Scale bars: 10 µm. (**E**,**J**) Quantification of mitochondrial network patterns. Data are the percentage of egg chambers showing the following mitochondrial network patterns: H, healthy networks as seen in healthy wild-type egg chambers; N, normal degeneration as seen in degenerating wild-type egg chambers; A, abnormal mitochondrial networks; I, abnormal networks with mitochondrial islands; *n*, the number of egg chambers analyzed.

regions of irregular follicle cell patterns (Fig. 8K), suggesting that the mCherry-DrAtg8a fusion could have some dominant-negative activity. The presence of these large follicle cell domains in *atg1* and *atg7* mutants, as well as in the *mcherry-Dratg8a* transgenic flies, suggests that the autophagy machinery is required for degradation in the follicle cells.

To further characterize the nature of the mitochondrial clusters, we examined whether the clusters are associated with acidic organelles by co-labeling egg chambers with LysoTracker and anti-ATP synthase. We found many LysoTracker-positive vesicles with mitochondria present and most of these were in the follicle cells (Fig. 9A-C). Additionally, we analyzed egg chambers by electron microscopy (Fig. 9D-H). We found that there were membrane-bound vesicles with dense nurse cell cytoplasm and mitochondrial clusters being taken up by the follicle cells (Fig. 9E) (Giorgi and Deri, 1976). Egg chambers later in degeneration showed vesicles containing mitochondria with discontinuous cristae and outer membranes (Fig. 9G,H). Our findings suggest that degradation of nurse cell mitochondria occurs predominantly in the surrounding follicle cells.

DISCUSSION

Here, we have shown that mitochondria undergo a stepwise progression of rearrangement, cluster formation and breakdown during cell death in the fly ovary. This caspase-dependent cell death pathway does not require the cell death initiators Reaper, Hid and Grim, the adaptor molecule Ark, or the initiator caspase Dronc (Baum et al., 2007; Peterson et al., 2007). Instead, we find a major role for Bcl-2 family proteins in controlling both mitochondrial dynamics and cell death in the ovary.

We found that the Bcl-2 family genes *buffy* and *debcl* regulate germline cell death in mid-oogenesis with both proteins acting pro-apoptotically and in an age-dependent manner. Mutations in either gene led to undead egg chambers, with surviving nurse cells and a disappearance of follicle cells. The frequency of the undead egg chambers was increased in double mutants, suggesting these Bcl-2 family members act redundantly within the ovary. Buffy was originally described as an anti-apoptotic Bcl-2 family member (Quinn et al., 2003; Sevrioukov et al., 2007), but a recent loss-of-function study indicates that Buffy can act pro-apoptotically to promote the cell death of microchaete glia (Wu et al., 2010). Synergism between *buffy* and *debcl* has not been reported for cell death phenotypes, but they were both found to promote autophagy in a *Drosophila* cell line (Hou et al., 2008). It is unclear why the Bcl-2 mutants showed a stronger disruption of cell death in older flies. It should be noted, however, that 10-20 day old flies are not particularly ‘old’ and are still highly reproductively active (Waskar et al., 2005). There are dramatic gene expression changes that occur with increasing fly age (Zhan et al., 2007), suggesting that an alternative pathway could regulate ovarian cell death during early adult life. It is intriguing that Debcl and Buffy show the highest degree of similarity with Bok, Bcl-2-related ovarian killer (Brachmann et al., 2000; Colussi et al., 2000; Igaki et al., 2000; Zhang et al., 2000), implicating an evolutionarily conserved role in the regulation of ovarian cell death. Indeed, follicular atresia in mammals shares many remarkable similarities with cell death in *Drosophila* mid-oogenesis (Krysko et al., 2008; Pritchett et al., 2009).

Mitochondrial events that occurred during cell death in mid-oogenesis included: (1) the remodeling of germline mitochondria, (2) cluster formation, (3) uptake by follicle cells and (4) degradation in the follicle cells. Previously mitochondrial fragmentation has been shown to occur upstream of effector caspases following an apoptotic stimulus (Wang and Youle, 2009). Similarly, we found that mitochondria were extensively remodeled in undead egg chambers in mutants of the effector caspase Dcp-1. Surprisingly, we found that overexpression of the caspase inhibitor Diap1 led to a complete block in remodeling in over 40% of egg chambers. Because Diap1 can inhibit initiator caspases as well as effector caspases, it is possible that remodeling occurs downstream of initiator caspases. We previously found that the initiator caspases Strica and Dronc act redundantly during cell death in oogenesis (Baum et al., 2007), but even a double mutant does not show a complete block in cell death in mid-oogenesis, unlike mutants of the effector caspase Dcp-1 (Laundrie et al., 2003). Alternatively, Diap1, an E3 ubiquitin ligase (Orme and Meier, 2009), could regulate non-caspase targets to control mitochondrial dynamics.

Interestingly, the Bcl-2 family proteins affected mitochondrial remodeling during cell death with abnormal networks and large masses of mitochondria. Mitochondrial networks in the undead egg

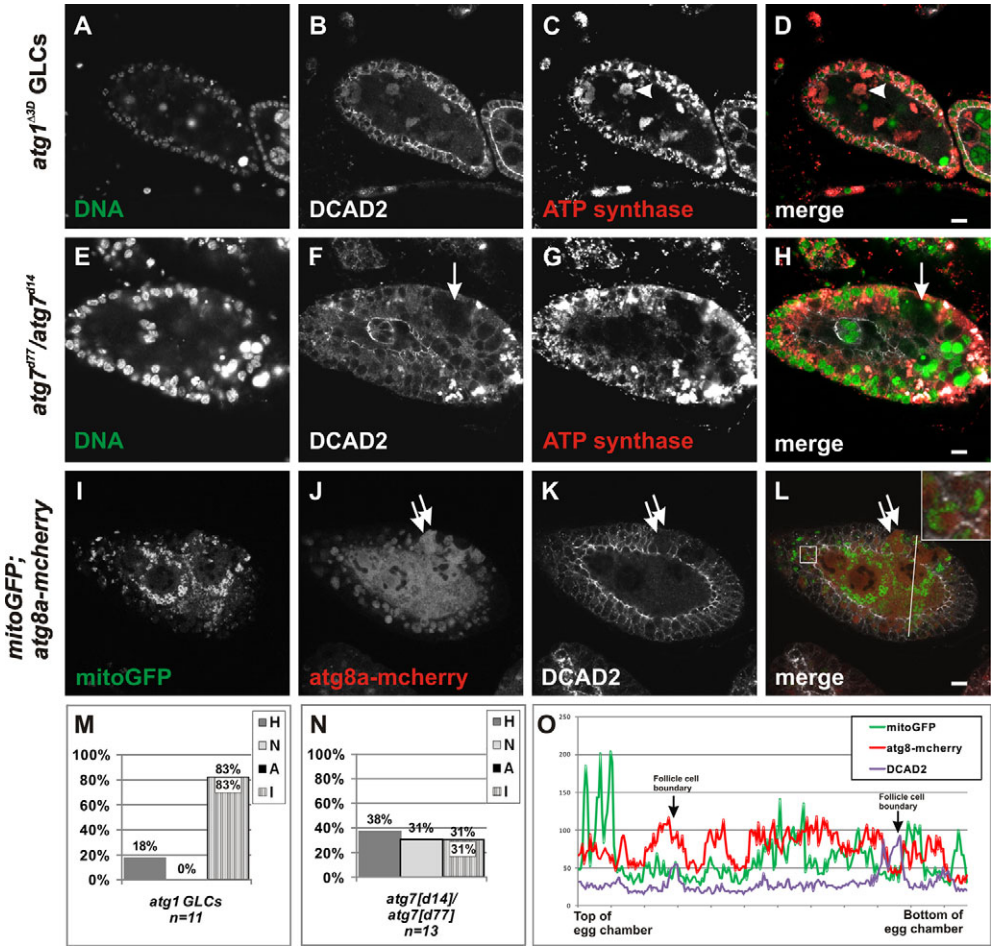

Fig. 8. The autophagic machinery affects mitochondrial remodeling and uptake by follicle cells. (**A-D**) An *atg1*$^{\Delta 3D}$ GLC degenerating egg chamber. (A) Nuclear morphology (DNA, OliGreen). (B) Follicle cell membranes visualized with anti-*Drosophila* e-cadherin (DCAD2, white). (C) Mitochondrial morphology (anti-ATP synthase, red). (D) Merge. Arrowhead indicates mitochondrial island. (**E-H**) An *atg7*^{d77}/*atg7*^{d14} degenerating egg chamber stained as in A-D. Arrow indicates large regions without staining, suggesting large vacuoles. DCAD2 was used to identify the borders around the follicle cells and between the follicle cells and the nurse cells. Bleed through between channels used to detect DCAD2 and ATP-synthase occurred but, based on control staining (DCAD2 alone), DCAD2 staining is not present at the site of mitochondrial clusters in the nurse cells or follicle cells (data not shown). (**I-L**) An egg chamber expressing (I) *UASp-mitoGFP* and (J) *UASp-mcherry-Dratg8a* driven in the germline by *NGT; nosGAL4* and stained with (K) anti-*Drosophila* e-cadherin (DCAD2). (L) Merge. Double arrows indicate large regions of discontinuous membrane. The inset in L is at 252× zoom. Scale bars: 10 μm. (**M**,**N**) Quantification of mitochondrial network patterns. Data are the percentage of degenerating egg chambers showing the following mitochondrial network patterns: H, healthy networks as seen in healthy wild-type egg chambers; N, normal degeneration as seen in degenerating wild-type egg chambers; A, abnormal mitochondrial networks; I, abnormal networks with mitochondrial islands; *n*, the number of egg chambers analyzed. (**O**) Line scan plot of the line drawn in L.

chambers were most similar to Diap1 overexpression, suggesting that the Bcl-2 family proteins act upstream of the first remodeling step. Additionally, we found that mitochondrial networks and cell death were disrupted in mutants of the mitochondrial fission and fusion genes, *drp1* and *opa1-like*. Mitochondrial networks in healthy egg chambers appeared as expected: *drp1* GLCs and flies with *opa1-like* overexpression had overly connected mitochondrial networks and *opa1-like* GLCs showed diffuse mitochondrial networks. *drp1* GLCs, *opa1-like* overexpression and *opa1-like* GLCs had disrupted cell death in mid-oogenesis. It was surprising that we saw the same effect on cell death regardless of whether mitochondrial fission or fusion were disrupted. Perhaps this is because Opa1-like acts both in fusion and fission events, or Opa1-like may have a direct pro-apoptotic role, as suggested by its role in cytochrome c release in mammals (Yamaguchi and Perkins, 2009). The striking similarity in phenotype between the Bcl-2 family proteins and the mitochondrial fission/fusion mutants suggests that they work together to regulate mitochondrial dynamics during cell death in mid-oogenesis.

After the initial mitochondrial remodeling step during cell death in mid-oogenesis, nurse cell mitochondria assembled into clusters. Formation of normal clusters was dependent on the effector caspase Dcp-1, on the Bcl-2 proteins, and on Drp1 and Atg1 (see below). In other *Drosophila* tissues and in other organisms, mitochondrial fragmentation occurs with the onset of cell death (Abdelwahid et al., 2007; Goyal et al., 2007; Suen et al., 2008), but the occurrence of mitochondrial clusters is unusual. Perhaps in the ovary, mitochondrial fragmentation initiates cell death but subsequent cluster formation is required for removal of the mitochondria, facilitating uptake by the follicle cells. The phagocytic removal of nurse cell remnants is unusual in that it occurs by packaging of vesicles of nurse cell cytoplasm, rather than

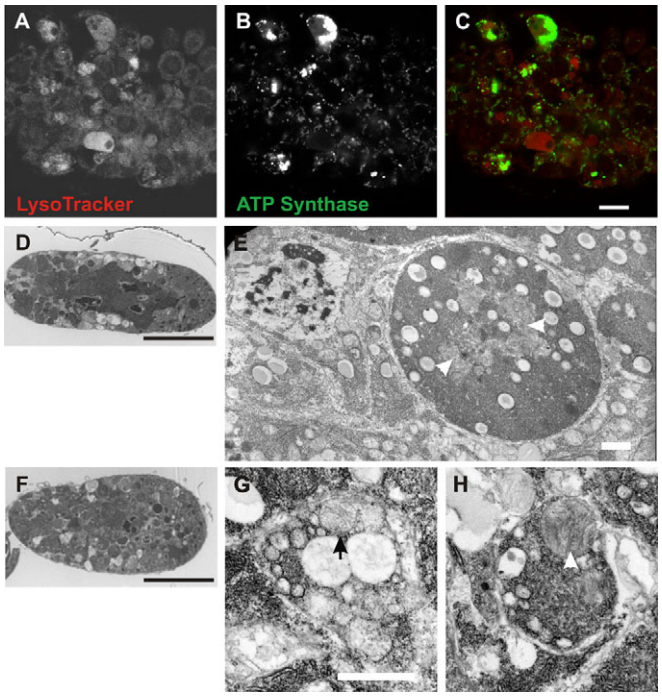

Fig. 9. Mitochondrial clusters colocalize with LysoTracker staining and can be seen in membrane-bound organelles by TEM. (**A-C**) A degenerating egg chamber stained with (A) LysoTracker and (B) anti-ATP synthase. (C) Overlay shows mitochondrial clusters (green) in LysoTracker-positive regions (red). Scale bar: 10 μm. (**D**,**F**) Degenerating wild-type stage 8 egg chambers. Sections (1 μm) stained with 1% Toluidine Blue showing overall morphology of egg chambers. Scale bars: 50 μm. (**E**) Electron micrograph of a region of the degenerating egg chamber in D. (**G**,**H**) Electron micrographs of the degenerating egg chamber in F. Arrow in G indicates a degenerating mitochondrion. Arrowheads in E and H indicate mitochondria. Scale bars: 1 μm in E,G.

phagocytosis of entire cells. The large size of the nurse cells relative to the follicle cells may require this atypical mechanism. Mitophagy, the degradation of mitochondria by autophagy, is thought to be a quality control process for maintaining healthy mitochondria (Twig et al., 2008). We found large mitochondrial masses (islands) in autophagy-deficient nurse cells, even in healthy egg chambers. This suggests that in the ovary, mitophagy maintains properly structured mitochondrial networks in healthy egg chambers. Similar mitochondrial masses have been reported in egg chambers from *clueless* and *parkin* mutants (Cox and Spradling, 2009). The aberrant islands found in autophagy mutant egg chambers persisted during degeneration, and mitochondrial remodeling during cell death was abnormal. Autophagy-deficient egg chambers show reduced TUNEL-labeling during cell death (Hou et al., 2008; Nezis et al., 2009); perhaps a mitochondrial factor could be required for DNA fragmentation.

In dying egg chambers, autophagy has been reported to be induced in nurse cells (Hou et al., 2008; Nezis et al., 2009). However, visualizing autophagy is complicated by the surrounding follicle cells that rapidly begin to engulf the nurse cell cytoplasm (Giorgi and Deri, 1976). Using follicle cell membrane markers, we find that most of the vesicles labeled by mCherry-DrAtg8a are actually in the follicle cells, and only in the follicle cells do we see substantial overlap between the autophagy marker and the mitochondrial clusters. Some of the egg chambers lacking Atg1 in the germline showed a delay in engulfment by the follicle cells, indicating that autophagy could be used to package germline cytoplasm for uptake by the follicle cells. We also observed large irregular follicle cells in the autophagy-deficient egg chambers, indicating that autophagy may play a role in proper degradation of nurse cell material once it is in the follicle cells.

Autophagy-deficient egg chambers were defective in mitochondrial remodeling during cell death, but did not proceed to an undead state (Hou et al., 2008; Nezis et al., 2009), in contrast to the Bcl-2 family and mitochondrial fission/fusion mutants. This suggests that the Bcl-2 proteins and mitochondrial fission/fusion machinery are required for a pro-apoptotic event(s) beyond mitochondrial remodeling. Cytochrome c release and MOMP are obvious candidates, analogous to mammalian models of cell death. We have not detected any evidence for cytochrome c exposure during cell death in mid-oogenesis (Peterson et al., 2007), but it is possible that other pro-apoptotic molecules are released. Alternatively, apoptosis-promoting factors may be specifically recruited to sites of mitochondrial fission (Oberst et al., 2008; Krieser and White, 2009). Our findings indicate that a cell death process decoupled from the IAP-binding proteins provides a powerful model for investigating mitochondrial control of cell death in *Drosophila*.

Acknowledgements
We thank Rachel Cox, Allan Spradling, Tom Neufeld, Iannis Nezis, Harald Stenmark, Hugo Bellen and the Bloomington Stock Center for fly strains. We thank Rachel Cox for helpful conversations, and Horacio Frydman, Michelle Cronin and members of the laboratory for comments on the manuscript. We thank Don Gantz at Boston University Medical Center for technical assistance with electron microscopy. This work was supported by NIH grant R01 GM060574 (K.M.), NICHD training grant 2T 32 HD007387 (E.T.) and a Career Award in the Biomedical Sciences from the Burroughs Wellcome Fund (C.B.B.). Deposited in PMC for release after 12 months.

Competing interests statement
The authors declare no competing financial interests.

Supplementary material
Supplementary material for this article is available at
http://dev.biologists.org/lookup/suppl/doi:10.1242/dev.057943/-/DC1

References

Abdelwahid, E., Yokokura, T., Krieser, R. J., Balasundaram, S., Fowle, W. H. and White, K. (2007). Mitochondrial disruption in *Drosophila* apoptosis. *Dev. Cell* **12**, 793-806.
Autret, A. and Martin, S. J. (2010). Bcl-2 family proteins and mitochondrial fission/fusion dynamics. *Cell. Mol. Life Sci.* **67**, 1599-1606.
Bass, B. P., Tanner, E. A., Mateos San Martin, D., Blute, T., Kinser, R. D., Dolph, P. J. and McCall, K. (2009). Cell-autonomous requirement for DNaseII in nonapoptotic cell death. *Cell Death Differ.* **16**, 1362-1371.
Baum, J. S., Arama, E., Steller, H. and McCall, K. (2007). The *Drosophila* caspases Strica and Dronc function redundantly in programmed cell death during oogenesis. *Cell Death Differ.* **14**, 1508-1517.
Brachmann, C. B., Jassim, O. W., Wachsmuth, B. D. and Cagan, R. L. (2000). The *Drosophila* Bcl-2 family member dBorg-1 functions in the apoptotic response to UV-irradiation. *Curr. Biol.* **10**, 547-550.
Colussi, P. A., Quinn, L. M., Huang, D. C., Coombe, M., Read, S. H., Richardson, H. and Kumar, S. (2000). Debcl, a proapoptotic Bcl-2 homologue, is a component of the *Drosophila melanogaster* cell death machinery. *J. Cell Biol.* **148**, 703-714.
Cox, R. T. and Spradling, A. C. (2003). A Balbiani body and the fusome mediate mitochondrial inheritance during *Drosophila* oogenesis. *Development* **130**, 1579-1590.
Cox, R. T. and Spradling, A. C. (2009). *clueless*, a conserved *Drosophila* gene required for mitochondrial subcellular localization, interacts genetically with *parkin*. *Dis. Model. Mech.* **2**, 490-499.
Dej, K. J. and Spradling, A. C. (1999). The endocycle controls nurse cell polytene chromosome structure during *Drosophila* oogenesis. *Development* **126**, 293-303.
Drummond-Barbosa, D. and Spradling, A. C. (2001). Stem cells and their progeny respond to nutritional changes during *Drosophila* oogenesis. *Dev. Biol.* **231**, 265-278.

Foley, K. and Cooley, L. (1998). Apoptosis in late stage *Drosophila* nurse cells does not require genes within the H99 deficiency. *Development* **125**, 1075-1082.
Frydman, H. M. and Spradling, A. C. (2001). The receptor-like tyrosine phosphatase *lar* is required for epithelial planar polarity and for axis determination within *Drosophila* ovarian follicles. *Development* **128**, 3209-3220.
Galindo, K. A., Lu, W.-J., Park, J. H. and Abrams, J. M. (2009). The Bax/Bak ortholog in *Drosophila*, Debcl, exerts limited control over programmed cell death. *Development* **136**, 275-283.
Giorgi, F. and Deri, P. (1976). Cell death in ovarian chambers of *Drosophila melanogaster*. *J. Embryol. Exp. Morphol.* **35**, 521-533.
Goldman, S. J., Taylor, R., Zhang, Y. and Jin, S. (2010). Autophagy and the degradation of mitochondria. *Mitochondrion* **10**, 309-315.
Goyal, G., Fell, B., Sarin, A., Youle, R. J. and Sriram, V. (2007). Role of mitochondrial remodeling in programmed cell death in *Drosophila melanogaster*. *Dev. Cell* **12**, 807-816.
Hou, Y. C., Chittaranjan, S., Barbosa, S. G., McCall, K. and Gorski, S. M. (2008). Effector caspase Dcp-1 and IAP protein Bruce regulate starvation-induced autophagy during *Drosophila melanogaster* oogenesis. *J. Cell Biol.* **182**, 1127-1139.
Igaki, T., Kanuka, H., Inohara, N., Sawamoto, K., Nunez, G., Okano, H. and Miura, M. (2000). Drob-1, a *Drosophila* member of the Bcl-2/CED-9 family that promotes cell death. *Proc. Natl. Acad. Sci. USA* **97**, 662-667.
Jagasia, R., Grote, P., Westermann, B. and Conradt, B. (2005). DRP-1-mediated mitochondrial fragmentation during EGL-1-induced cell death in *C. elegans*. *Nature* **433**, 754-760.
Juhasz, G., Erdi, B., Sass, M. and Neufeld, T. P. (2007). Atg7-dependent autophagy promotes neuronal health, stress tolerance, and longevity but is dispensable for metamorphosis in *Drosophila*. *Genes Dev.* **21**, 3061-3066.
Karbowski, M., Lee, Y. J., Gaume, B., Jeong, S. Y., Frank, S., Nechushtan, A., Santel, A., Fuller, M., Smith, C. L. and Youle, R. J. (2002). Spatial and temporal association of Bax with mitochondrial fission sites, Drp1, and Mfn2 during apoptosis. *J. Cell Biol.* **159**, 931-938.
King, R. C. (1970). *Ovarian Development in Drosophila melanogaster*. New York: Academic Press.
Krieser, R. and White, K. (2009). Inside an enigma: do mitochondria contribute to cell death in *Drosophila*? *Apoptosis* **14**, 961-968.
Krysko, D., Diez-Fraile, A., Criel, G., Svistunov, A., Vandenabeele, P. and D'Herde, K. (2008). Life and death of female gametes during oogenesis and folliculogenesis. *Apoptosis* **13**, 1065-1087.
Laundrie, B., Peterson, J. S., Baum, J. S., Chang, J. C., Fileppo, D., Thompson, S. and McCall, K. (2003). Germline cell death in inhibited by P element insertions in the *dcp-1/pita* nested gene pair in *Drosophila*. *Genetics* **165**, 1881-1888.
Mazzalupo, S. and Cooley, L. (2006). Illuminating the role of caspases during *Drosophila* oogenesis. *Cell Death Differ.* **13**, 1950-1959.
Nezis, I. P., Lamark, T., Velentzas, A. D., Rusten, T. E., Bjorkoy, G., Johansen, T., Papassideri, I. S., Stravopodis, D. J., Margaritis, L. H., Stenmark, H. et al. (2009). Cell death during *Drosophila melanogaster* early oogenesis is mediated through autophagy. *Autophagy* **5**, 298-302.
Oberst, A., Bender, C. and Green, D. R. (2008). Living with death: the evolution of the mitochondrial pathway of apoptosis in animals. *Cell Death Differ.* **15**, 1139-1146.
Orme, M. and Meier, P. (2009). Inhibitor of apoptosis proteins in *Drosophila*: gatekeepers of death. *Apoptosis* **14**, 950-960.
Park, J., Lee, S. B., Lee, S., Kim, Y., Song, S., Kim, S., Bae, E., Kim, J., Shong, M., Kim, J.-M. et al. (2006). Mitochondrial dysfunction in *Drosophila* PINK1 mutants is complemented by *parkin*. *Nature* **441**, 1157-1161.
Peterson, J. S., Barkett, M. and McCall, K. (2003). Stage-specific regulation of caspase activity in *Drosophila* oogenesis. *Dev. Biol.* **260**, 113-123.
Peterson, J. S., Bass, B. P., Jue, D., Rodriguez, A., Abrams, J. M. and McCall, K. (2007). Noncanonical cell death pathways act during *Drosophila* oogenesis. *Genesis* **45**, 396-404.
Pritchett, T. L., Tanner, E. A. and McCall, K. (2009). Cracking open cell death in the *Drosophila* ovary. *Apoptosis* **14**, 969-979.
Quinn, L., Coombe, M., Mills, K., Daish, T., Colussi, P., Kumar, S. and Richardson, H. (2003). Buffy, a *Drosophila* Bcl-2 protein, has anti-apoptotic and cell cycle inhibitory functions. *EMBO J.* **22**, 3568-3579.
Rolland, S. G., Lu, Y., David, C. N. and Conradt, B. (2009). The BCL-2-like protein CED-9 of *C. elegans* promotes FZO-1/Mfn1,2- and EAT-3/Opa1-dependent mitochondrial fusion. *J. Cell Biol.* **186**, 525-540.
Scott, R. C., Juhasz, G. and Neufeld, T. P. (2007). Direct induction of autophagy by Atg1 inhibits cell growth and induces apoptotic cell death. *Curr. Biol.* **17**, 1-11.
Sevrioukov, E. A., Burr, J., Huang, E. W., Assi, H. H., Monserrate, J. P., Purves, D. C., Wu, J. N., Song, E. J. and Brachmann, C. B. (2007). *Drosophila* Bcl-2 proteins participate in stress-induced apoptosis, but are not required for normal development. *Genesis* **45**, 184-193.
Suen, D. F., Norris, K. L. and Youle, R. J. (2008). Mitochondrial dynamics and apoptosis. *Genes Dev.* **22**, 1577-1590.
Twig, G., Hyde, B. and Shirihai, O. S. (2008). Mitochondrial fusion, fission and autophagy as a quality control axis: The bioenergetic view. *Biochim. Biophys. Acta* **1777**, 1092-1097.
Velentzas, A. D., Nezis, I. P., Stravopodis, D. J., Papassideri, I. S. and Margaritis, L. H. (2007). Apoptosis and autophagy function cooperatively for the efficacious execution of programmed nurse cell death during *Drosophila virilis* oogenesis. *Autophagy* **3**, 130-132.
Verstreken, P., Ly, C. V., Venken, K. J., Koh, T. W., Zhou, Y. and Bellen, H. J. (2005). Synaptic mitochondria are critical for mobilization of reserve pool vesicles at *Drosophila* neuromuscular junctions. *Neuron* **47**, 365-378.
Wang, C. and Youle, R. J. (2009). The role of mitochondria in apoptosis. *Annu. Rev. Genet.* **43**, 95-118.
Waskar, M., Li, Y. and Tower, J. (2005). Stem cell aging in the *Drosophila* ovary. *Age* **27**, 201-212.
Wu, J. N., Nguyen, N., Aghazarian, M., Sevrioukov, E. A., Monserrate, J. P., Tang, W., Mabuchi, M., Tan, Y., White, K. and Brachmann, C. B. (2010). *grim* promotes programmed cell death of *Drosophila* microchaete glial cells. *Mech. Dev.* **127**, 407-417.
Xu, D., Woodfield, S. E., Lee, T. V., Fan, Y., Antonio, C. and Bergmann, A. (2009). Genetic control of programmed cell death (apoptosis) in *Drosophila*. *Fly* **3**, 78-90.
Yamaguchi, R. and Perkins, G. (2009). Dynamics of mitochondrial structure during apoptosis and the enigma of Opa1. *Biochim. Biophys. Acta* **1787**, 963-972.
Zhan, M., Yamaza, H., Sun, Y., Sinclair, J., Li, H. and Zou, S. (2007). Temporal and spatial transcriptional profiles of aging in *Drosophila* melanogaster. *Genome Res.* **17**, 1236-1243.
Zhang, H., Huang, Q., Ke, N., Matsuyama, S., Hammock, B., Godzik, A. and Reed, J. C. (2000). *Drosophila* pro-apoptotic Bcl-2/Bax homologue reveals evolutionary conservation of cell death mechanisms. *J. Biol. Chem.* **275**, 27303-27306.